Two- to One-Dimensional: Radii-Dependent Self-Assembly Crystal Structures and Luminescent Properties of Lanthanide Coordination Polymers with an Amide Type Semirigid Bridging Ligan...

10 AUTHORS, INCLUDING:

Xiaoguang Huang
Lanzhou University
6 PUBLICATIONS **79** CITATIONS

Yu Tang
Lanzhou University
96 PUBLICATIONS **821** CITATIONS

Two- to One-Dimensional: Radii-Dependent Self-Assembly Crystal Structures and Luminescent Properties of Lanthanide Coordination Polymers with an Amide Type Semirigid Bridging Ligand

Xuhuan Yan, Yafei Li, Qiong Wang, Xiaoguang Huang, Ye Zhang, Cunji Gao, Weisheng Liu, Yu Tang,* Hongrui Zhang, and Yongliang Shao

Key Laboratory of Nonferrous Metal Chemistry and Resources Utilization of Gansu Province, State Key Laboratory of Applied Organic Chemistry and College of Chemistry and Chemical Engineering, Lanzhou University, Lanzhou 730000, People's Republic of China

S *Supporting Information*

ABSTRACT: Lanthanide coordination polymers $\{[Ln_2L_3(NO_3)_6]\cdot nH_2O\}_n$ [Ln = Pr (**1**), Nd (**2**), Sm (**3**), Eu (**4**), Gd (**5**), Tb (**6**), Dy (**7**), and Er (**8**), where $n = 0$ except for **1** with $n = 4$ and **2** with $n = 7$] have been assembled using lanthanide nitrates and an amide type semirigid bridging ligand, 1,3-bis{[(2′-benzylaminoformyl)phenoxyl]methylbenzene (L), as building blocks. The crystal structures of the complexes $\{[Pr_2L_3(NO_3)_6]_n\cdot 4H_2O\}_n$ (**1**), $\{[Nd_2L_3(NO_3)_6]\cdot 7H_2O\}_n$ (**2**), $[Sm_2L_3(NO_3)_6]_n$ (**3**), $[Eu_2L_3(NO_3)_6]_n$ (**4**), $[Tb_2L_3(NO_3)_6]_n$ (**6**), and $[Er_2L_3(NO_3)_6]_n$ (**8**)} were determined by single-crystal X-ray diffraction. Interestingly, **1** and **2** demonstrate unusual lanthanide porous noninterpenetrated honeycomb-like (6,3) topology frameworks, while **3**, **4**, **6**, and **8** exhibit novel one-dimensional linear coordination polymeric structures. Their structural variations are attributed to lanthanide contraction effects. The luminescent properties of Sm(III), Eu(III), Tb(III), and Dy(III) complexes are also investigated in detail. The lowest triplet state (T_1) energy level of this ligand matches better to the lowest resonance energy levels of Tb(III) and Dy(III) than Eu(III) and Sm(III) ions.
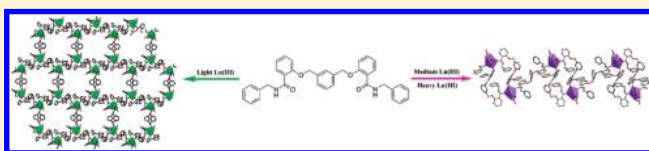
■ INTRODUCTION

The design and assembly of coordination polymers have been of considerable interest because of their potential applications, such as gas storage, sensor, separation, catalysis, ion exchange, and other materials applications.[1] However, many coordination polymers reported previously were mainly based on transition metals. As compared with transition metal centers, the lanthanide ions have much higher coordination numbers and more flexible coordination geometry, which make them difficult to control or predict the network architectures of the lanthanide coordination polymers but are helpful in the formation of novel supramolecular architectures dictated by the different size of the lanthanide ions, such as 1D chains, 2D grids, 3D porous structures, and interpenetrated networks.[2] Generally, the lanthanide series can be divided into three groups according to their masses: the light La-Pm, the medium Sm-Dy, and the heavy Ho-Lu. The radii of the lanthanide cations decrease with increasing atomic number, which imposes evident influences on the coordination geometry and might lead to different types of network and physical properties. Thus, it is interesting to investigate whether the architecture is maintained across the lanthanide series. In addition, lanthanide ions can exhibit excellent photophysical properties; especially, Sm(III), Eu(III), Tb(III), and Dy(III) are, in general, considered to have the brightest emission with some organic ligands, which play a vital role in sensors, liquid crystalline materials, or luminescent labeling reagents for specific biomolecular interactions.[3] To obtain fascinating topological
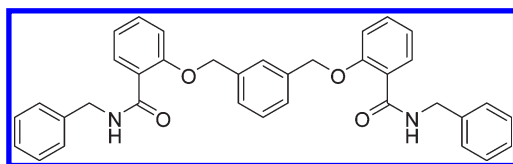
structures as well as satisfactory luminescent properties, selecting ligand suitably is the key factor. Ligand designs have been mainly based on structures that can encapsulate the lanthanide ions such as macrocycles and cryptands,[4] podands,[5] or shell type ligands,[6] imposing bulkiness around the metal ions. Amide type ligands are excellent candidates due to their selective coordinating capacity, spheroidal cavities, and hard binding sites, therefore stabilizing their complexes, acquiring novel coordination structures, and shielding the encapsulated metal ions from interaction with the surroundings effectively and exhibiting exceptional luminescent properties.[2g,4a,7] Our group has been interested in employing self-assembly strategies for lanthanide complexes and has recently selected amide type ligands as organic molecular building blocks to construct the novel and satisfactory luminescent lanthanide-organic frameworks (LnOFs). As a part of our systematic studies, this paper reports the radii-dependent self-assembly and luminescent properties of lanthanide coordination polymers with an amide type semirigid bridging ligand 1,3-bis{[(2′-benzylaminoformyl)phenoxyl]methyl}benzene (L, Scheme 1). This ligand and the crystal structure of the Eu(III) nitrate complex have previously been reported by us.[2g] In this report, the crystal analysis unambiguously reveals that compounds $\{[Pr_2L_3(NO_3)_6]_n\cdot 4H_2O\}_n$ (**1**) and $\{[Nd_2L_3(NO_3)_6]\cdot 7H_2O\}_n$ (**2**) form unusual

Scheme 1. Schematic Illustration of the Ligand L

Table 1. Elemental Analytical and IR Spectral Data of the Complexes

complexes	found (calcd) (%)			IR (cm^{-1})
	C	H	N	$\nu(C{=}O)$
$[Pr_2L_3(NO_3)_6]\cdot 2H_2O$	54.82 (54.97)	3.88 (4.27)	6.74 (7.12)	1606
$[Nd_2L_3(NO_3)_6]\cdot 2H_2O$	54.75 (54.81)	3.87 (4.26)	6.72 (7.10)	1607
$[Sm_2L_3(NO_3)_6]\cdot 2H_2O$	54.42 (54.53)	3.88 (4.24)	6.73 (7.07)	1608
$[Gd_2L_3(NO_3)_6]\cdot 2H_2O$	54.18 (54.22)	3.85 (4.21)	6.78 (7.03)	1610
$[Tb_2L_3(NO_3)_6]\cdot 2H_2O$	54.09 (54.14)	3.84 (4.21)	6.74 (7.02)	1612
$[Dy_2L_3(NO_3)_6]\cdot 2H_2O$	54.00 (53.98)	4.16 (4.19)	6.96 (6.99)	1611
$[Er_2L_3(NO_3)_6]\cdot 2H_2O$	53.74 (53.77)	4.18 (4.16)	6.97 (6.95)	1613

lanthanide porous noninterpenetrated two-dimensional (2D) honeycomb-like $(6,3)^{2i,8}$ (hcb, Schläfli symbol $6,^3$ vertex symbol $6\cdot6\cdot6$) topology networks, which are, to our best knowledge, an unusual net of lanthanide coordination polymers.[2f,i,7b−7d,9] However, compounds $[Sm_2L_3(NO_3)_6]_n$ (**3**), $[Eu_2L_3(NO_3)_6]_n$ (**4**),[2g] $[Tb_2L_3(NO_3)_6]_n$ (**6**), and $[Er_2L_3(NO_3)_6]_n$ (**8**) exhibit novel one-dimensional (1D) coordination polymeric structures comprised of dinuclear metallorings connected by ligands under the same conditions. The structures of these six lanthanide coordination polymers clearly reflect the effect of the lanthanide contraction. So far, little attention was paid to the diversity of the topological structure of lanthanide coordination polymers controlled by lanthanide contraction effect.[10] Moreover, the luminescent properties of the Sm(III), Eu(III), Tb(III), and Dy(III) complexes were also studied in detail.

■ EXPERIMENTAL SECTION

Materials and Instrumentation. *N*-Benzylsalicylamide[11] was prepared according to the literature method. Lanthanide nitrates were prepared by the reaction of lanthanide oxides and nitric acid (7 mol L^{-1}), and then, superfluous nitric acid was removed. Other chemicals were obtained from commercial sources and used without further purification. Elemental analysis was determined on an Elementar Vario EL analyzer. The Fourier transform infrared (FT-IR) spectra were recorded on a Nicolet 360 FT-IR spectrometer using KBr pellets in the range of 4000−400 cm^{-1}. The ^{1}H NMR spectrum was measured on a Varian Mercury-300B spectrometer in *d*-chloroform solution with tetramethylsilane $[Si(CH_3)_4]$ as an internal standard. The solid state luminescence spectra of Sm(III), Eu(III), Tb(III), and Dy(III) complexes [the excitation and emission slit widths were 1.0 and 1.0 nm except for the Sm(III) complex with the excitation and emission slit widths being 2.5 and 1.0 nm] and the phosphorescence spectrum of Gd (III) complex were obtained on a Hitachi F-4500 fluorescence spectrophotometer. UV/vis absorption spectra were determined on a Varian UV-Cary100 spectrophotometer. Thermogravimetric analysis (TGA) was performed under N_2 atmosphere with a heating rate of 10 °C/min on a LINSEIS STA PT1600 thermal analyzer. Powder X-ray diffraction patterns (PXRD) were determined with a Rigaku-Dmax 2400 diffractometer using Cu Kα radiation. The overall luminescence quantum yields of the complexes were determined by an absolute method using an integrating sphere (150 mm diameter, $BaSO_4$ coating) from Edinburgh Instruments FLS920. The lifetime measurement was measured on an Edinburgh Instruments FLS920 Fluorescence Spectrometer with Nd pumped OPOlette laser as the excitation source.

Preparation of the Ligand L. The synthetic route of the ligand 1,3-bis{[(2′-benzylaminoformyl)phenoxyl]methyl}benzene (L) was reported in our previous paper.[2g]

Preparation of the Lanthanide Complexes. A solution of 0.15 mmol L in 10 cm^3 of ethyl acetate was added dropwise to a solution of 0.1 mmol $Ln(NO_3)_3\cdot 6H_2O$ (RE = Pr, Nd, Sm, Eu, Gd, Tb, Dy, and Er) in 10 cm^3 of ethyl acetate. The mixture was stirred at room temperature for 4 h. Then, diethyl ether was added to the mixture, and the precipitated solid complex was filtered, washed with ethyl acetate and diethyl ether, and dried in vacuo over P_4O_{10} for 48 h and submitted for elemental analysis,

yield 63−70%. Elemental analytical and IR spectral data for the newly synthesized complexes are summarized in Table 1. Single crystals of Pr, Nd, Sm, Eu, Tb, and Er complexes were grown from the mixed solution of ethyl acetate and chloroform (v:v = 1:1) with slow evaporation for 3 weeks at room temperature.

X-ray Crystallographic. The X-ray single-crystal data collection for complexes was performed on a Bruker Smart CCD diffractometer, using graphite-monochromated Mo Kα radiation (λ = 0.71073 Å). Semiempirical absorption corrections were applied using the SADABS program. The structures were solved by direct methods and refined by full-matrix least-squares on F^2 using the SHELXS-97 and SHELXL-97 programs.[12] All nonhydrogen atoms were refined anisotropically by full-matrix least-squares methods on F^2. Primary nonhydrogen atoms were solved by direct method, and secondary nonhydrogen atoms were solved by difference maps. The hydrogen atoms were added geometrically and not refined. CCDC-668262 [Pr(III) complex], 819659 [Nd(III) complex], 819660 [Sm(III) complex], 668261 [Eu(III) complex],[2g] 819661 [Tb(III) complex], and 819662 [Er(III) complex] contain the supplementary crystallographic data for this paper, which can be obtained free of charge from The Cambridge Crystallographic Data Centre via www.ccdc.cam.ac.uk/data_request/cif.

■ RESULTS AND DISCUSSION

Synthesis and Characterization. The lanthanide complexes were synthesized by the reaction of lanthanide nitrates with an amide type semirigid bridging ligand, 1,3-bis{[(2′-benzylamino-formyl)phenoxyl]methyl}benzene (L), in ethyl acetate. The obtained complexes are highly stable in air. Elemental analytical and IR spectral data for all of the complexes are summarized in Table 1. The solid powders of the complexes are soluble in DMF, DMSO, methanol, ethanol, and acetone, slightly soluble in acetonitrile but insoluble in $CHCl_3$ and diethyl ether. The IR spectrum of the free ligand displays characteristic absorption of carbonyl group at 1644 cm^{-1}. As compared to the free ligand, the absence of the band 1644 cm^{-1}, which is instead by a new band at ca. 1610 cm^{-1} of the complexes, indicates that the oxygen atom of the carbonyl group takes part in coordination to the metal ions. Single crystals of the Pr(III) (**1**), Nd(III) (**2**), Sm(III) (**3**), Eu(III) (**4**), Tb(III) (**6**), and Er(III) (**8**) complexes were grown from the mixed solution of ethyl acetate and chloroform (v:v = 1:1)
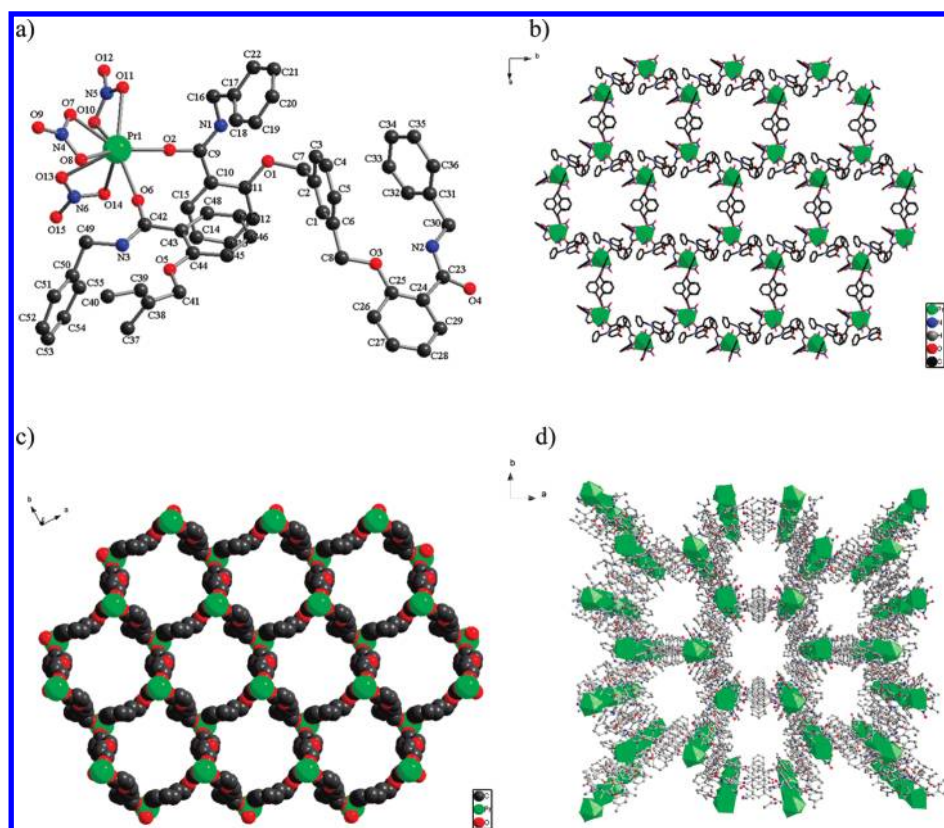
Figure 1. (a) Coordination sphere of the Pr(III) ion in **1**. (b) The crystal unit packing arrangement of **1**. (c) The simplified crystal unit packing arrangement of **1**. (d) View of 3D noninterpenetrated honeycomb-like layers of (6,3) topology with 1D channels along the *c*-axis of **1**. The hydrogen atoms, nitrates, and benzene rings of branched chain, benzylamine groups of the ligands, and the crystallization water molecules are omitted for clarity.

with slow evaporation for 3 weeks at room temperature. Crystallographic data as well as details of data collection and refinement for these complexes are summarized in the Supporting Information (Table S1), and important bond lengths and bond angles are listed in the Supporting Information (Table S2). Hydrogen bonds in crystal packing for the compounds **1**, **2**, **3**, **6**, and **8** are listed in the Supporting Information (Table S3).

Crystal Structures Descriptions. *Crystal Structures of the Compounds **1** and **2**.* The single-crystal X-ray analysis reveals that **1** and **2** possess the same space group and similar cell parameters (see Table S1 in the Supporting Information), which indicate that complexes $\{[Pr_2L_3(NO_3)_6]_n \cdot 4H_2O\}_n$ (**1**) and $\{[Nd_2L_3(NO_3)_6] \cdot 7H_2O\}_n$ (**2**) possess the same topological structures despite the fact that four crystallization water molecules that occurs in **1** was replaced by seven crystallization water molecules in **2**. Herein, only **1** is selected for investigation in detail as a representative example. The single-crystal structure of **1** shows that the Pr(III) ion has a nine-coordinate environment, six of which are occupied by six oxygen atoms from three bidentate nitrate groups, and the remaining three sites are occupied by the oxygen atoms of carbonyl groups of three bridging ligands (Figure 1a), forming a distorted tricapped trigonal prism. At the same time, each ligand binds to two Pr(III) ions using its two oxygen atoms of the carbonyl groups in *trans*-conformation. So, the whole structure consists of 2D (6,3) networks extending in the *ab* plane, in which the Pr centers provide the three-connecting nodes with essentially trigonal prism geometry and the bridging ligands connect pairs of Pr centers, as can be seen in Figure 1b. Each hexagon is defined by

six Pr centers as its vertices and six bridging ligands as its edges, and the adjacent rings share edges and vertices to form a 2D honeycomb lattice. The six Pr centers form the vertices of two triangles: One triangle is defined by the vertices at positions 1, 3, and 5, while the other is defined by the vertices at positions 2, 4, and 6 (Figure 1c). These two triangles are parallel to one another and approximately 12.79 Å apart. In the present case, the (6,3) net is not the ubiquitous flat graphene sheet but a topologically equivalent (6,3) net of chair conformation six rings, which forms a coordination polymer analogue of the puckered layers in graphite monofluoride, CF_x.[13] Furthermore, the corrugated honeycomb layers are stacked in an AAA manner along the *c*-axis by extensive intermolecular hydrogen bonds (Table S3 in the Supporting Information), resulting in a noninterpenetrated three-dimensional (3D) hexagonal channel (Figure 1d). Calculation using PLATON[14] reveals that the solvent-accessible portion accounts for about 41.2% of the crystal volume. In addition, all of the anions, NO_3^-, do not lie in cavities within the network but bind to the Pr(III), so that the whole frame is a completely neutral network. Up to now, the assembly of a honeycomb-like structure is challenging since the hexagon represents the most common pattern in nature and is familiar from benzene to the honeycomb of the bee. It is uncommon to generate honeycomb-like networks using the amide type semirigid bridging ligand. Especially, in this complex, the "all-chair" 2D honeycomb network that is structurally analogous to CF_x is rare. To our best knowledge, this type of lanthanide noninterpenetrated neutral (6,3) topological frameworks having large macrometallocycles constructed by amide ligand is few. To study the thermal stability
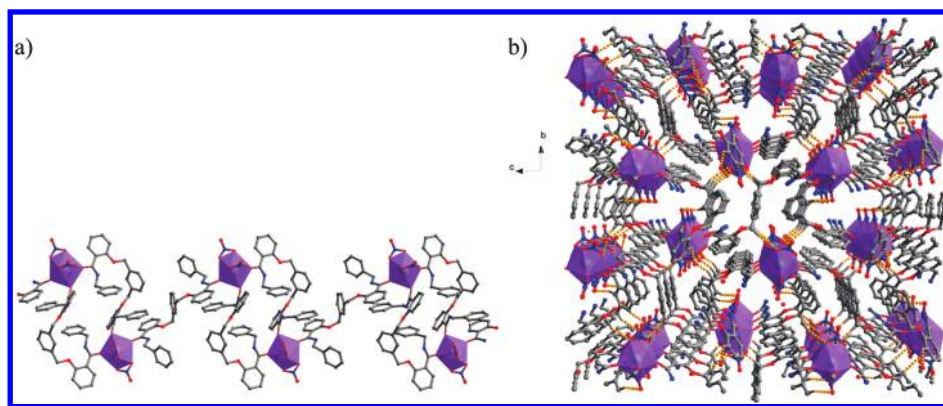
Figure 2. (a) One-dimensional rings connected by chains coordination polymer of **3**. (b) Three-dimensional supramolecular structure of **3** generated by intermolecular hydrogen bonds. The hydrogen atoms without formed hydrogen bonds and the benzyl groups of the ligands are omitted for clarity.

of **1**, TGA was performed on polycrystalline sample (Figure S1 in the Supporting Information). The crystallization water molecules were completely lost at 210 °C for **1** (calcd/found = 3.01/2.96%). Moreover, **1** was selected to examine the experimental variable-temperature PXRD after calcination at the temperature range of room temperature to 180 °C. The experimental PXRD patterns of **1** were still in agreement with the simulated one at 170 °C, indicating that the crystal lattice of **1** remains intact at 170 °C (Figure S2 in the Supporting Information). When the sample of **1** was heated at 180 °C, the structure formed amorphous phase.

*Crystal Structures of Compounds **3**, **4**, **6**, and **8***. These four complexes are isostructural. The coordination polyhedra around Sm(III), Eu(III), Tb(III), and Er(III) are all distorted tricapped trigonal prisms. They exhibit novel 1D coordination polymeric structures comprised of dinuclear metallorings connected by ligands. Herein, the structure of complex **3** was shown in Figure 2a, which is similar to our reported structure of compound **4**.[2g]

In complex **3**, atoms C(13), C(21), C(22), and C(51) of the ligand L act as hydrogen bond donors to form O···H−C with the oxygen atoms O(8), O(11), O(15), and O(9) of a neighboring molecule, thus generating a 3D porous supramolecular network (Figure 2b). The porosity is a very important property for coordination polymers. However, unfortunately, the ligands fill the channels themselves with their "thick" rods and large terminal groups in this compound, resulting in the volume of cavities that is only 4.6%. All of the relevant hydrogen-bonding values and symmetry codes are listed in Table S3 in the Supporting Information.

Comparison of the Structures. For further careful investigation of the self-assembly between lanthanide nitrates and the amide type bridging ligand, six coordination polymers were isolated. These six polymers have the same crystal system of monoclinic, but they exhibit two different kinds of crystal structures. For **1** and **2**, which form 2D porous noninterpenetrated honeycomb-like (6,3) frameworks, the lanthanide atoms [Pr (**1**) and Nd (**2**)] belong to the light lanthanide. The lanthanide atoms [Sm (**3**), Eu (**4**), Tb (**6**), and Er (**8**)] of **3**, **4**, **6**, and **8**, which exhibit special 1D linear coordination polymeric structures comprised of dinuclear metallorings connected by ligands, belong to the medium lanthanide and the heavy lanthanide. The average lengths of lanthanide and O atoms of these complexes are 2.500 and 2.482 Å for complexes **1** and **2** and 2.459, 2.448, 2.418, and 2.394 Å for **3**, **4**, **6**, and **8**, steadily

decreasing from Pr(III) to Er(III), respectively, which can be explained by the decrease in the respective effective ionic radii of the central lanthanide ion [1.18 Å for Pr(III), 1.16 Å for Nd(III), 1.13 Å for Sm(III), 1.12 Å for Eu(III), 1.10 Å for Tb(III), and 1.06 Å for Er(III)]. Moreover, a deeper view of the two kinds of different coordination polymers indicates that there are two crystallographically independent ligand conformations in all complexes. Herein, **1** and **3** are representatively discussed in detail. In compound **1**, the ether oxygen atoms (O1, O3, and O5) and oxygen atoms (O2, O4, and O6) of the carbonyl groups of two ligands adopt divergent *trans*-conformations. However, in compound **3**, the ether oxygen atoms (O5) and oxygen atoms (O6) of carbonyl groups of one ligand adopt divergent *trans*-conformation, and the ether oxygen atoms (O2 and O3) and oxygen atoms (O1 and O4) of carbonyl groups of the other ligand adopt a gathered-round *cis*-conformation. It is the lanthanide contraction effect that results in forming the different crystal structures. The coordination numbers of all compounds are nine. So, under the same conditions of the coordination numbers, with the increasing atomic number of lanthanide, to coordinate with lanthanide ions effectively, the ligands in **1** and **2** adopted divergent *trans*-conformations were converted to one gathered-round *cis*-conformation and the other divergent *trans*-conformation in **3**, **4**, **6**, and **8** (Figure 3). There are also strong intramolecular hydrogen bonds between the amide nitrogen atoms (N1, N2, and N3) and the ether oxygen atoms (O1, O2, O3, O5, and O6) in compounds **1** and **3** (Figure 3), which may have template effect and participate in the stabilization of the complex architectures and enhance the luminescent properties.

In these complexes, requirement of high coordination numbers of the lanthanide ion is satisfied by three bridging ligands and three bidentate nitrate groups. This prevents coordinated solvent molecules, especially water or alcohol from quenching lanthanide luminescence. So, the ability of the ligands to satisfy the coordination requirements of the Ln(III) centers with high coordination numbers becomes an important criterion in the design of supramolecular photonic devices.[15]

Electronic Absorption Spectra. The electronic spectra in the visible region of the Ln(III) complexes exhibit alternations in intensity and shifts in position of the absorption bands relative to the corresponding Ln(III) aquo ions. The shifts are due to the nephelauxetic effect and are regarded as a measure of covalency of bonding between the metal and the ligands. The spectroscopic covalent parameters of the Ln(III)-ligand bonds generally were
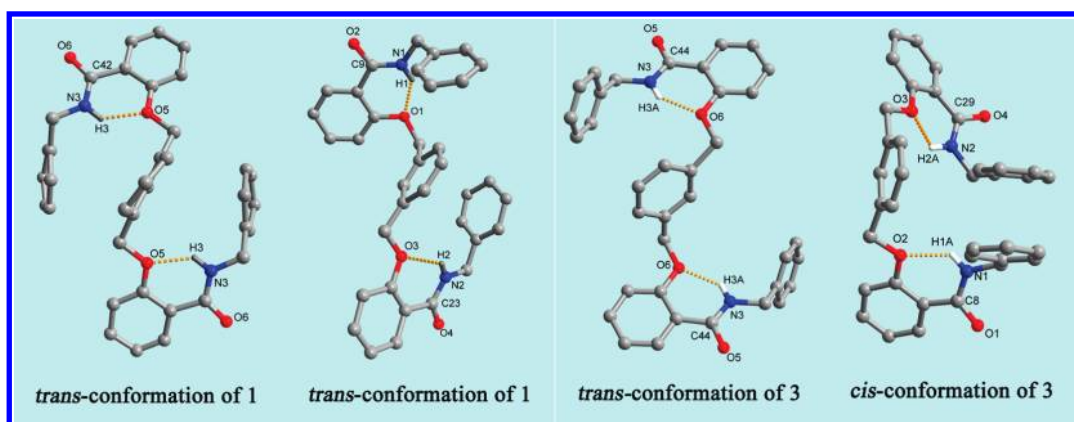
Figure 3. View of the conformations of ligand in complexes **1** and **3**. The hydrogen atoms without formed hydrogen bonds are omitted for clarity.

Table 2. Electronic Absorption Spectral Data and Covalent Parameters of 1, 2, and 8

complexes	frequency (cm^{-1})^a	assignment	covalence parameters
1	21231 (21255)	$^3H_4 \rightarrow {}^1I_6$	$\beta = 0.995$
	20790 (21085)	$^3H_4 \rightarrow {}^3P_1$	$\delta = 0.503$
	16611 (16595)	$^3H_4 \rightarrow {}^1D_2$	$b^{1/2} = 0.0500$
2	17216 (17203)	$^4I_{9/2} \rightarrow {}^2G_{7/2}$	$\beta = 0.997$
	13359 (13435)	$^4I_{9/2} \rightarrow {}^4S_{3/2}$	$\delta = 0.301$
	12545 (12608)	$^4I_{9/2} \rightarrow {}^2H_{9/2}$	$b^{1/2} = 0.0387$
8	20535 (20313)	$^4I_{15/2} \rightarrow {}^4F_{7/2}$	$\beta = 1.01$
	19196 (19147)	$^4I_{15/2} \rightarrow {}^2H_{11/2}$	$\delta = -0.990$
	15336 (15136)	$^4I_{15/2} \rightarrow {}^4F_{9/2}$	

^{a} The frequencies in parentheses are the electronic spectroscopic data for the corresponding Ln(III)−aquo ions.

assessed by the nephelauxetic ratio (β), Sinha's parameter (δ), and bonding parameter ($b^{1/2}$) (see the Supporting Information).[16] Absorption spectra of the **1**, **2**, and **8** were registered in methanol solutions at room temperature, and the covalent parameters were calculated and listed in Table 2. The values of β, δ, and $b^{1/2}$ are calculated to explain the nature of complexation. We have observed that the β values increase from Pr(III) to Er(III), indicating a decrease in covalent character and an increase in ionoic character of the metal−ligand bonds in the heavier lanthanide complexes (in agreement with the lanthanide contraction).

Luminescent Properties of the Complexes. The photoluminescence mechanism of the lanthanide complexes is proposed as a ligand-sensitized luminescence process (antenna effect).[17] In this process, the efficient energy transfer from ligand to central ions is one of key factors to achieve lanthanide characteristic luminescence.[18]

Excited by the absorption band at 323 nm, the "free" ligand exhibits broad emission bands (λ_{max} = 444 nm), and the solid state excitation and emission spectra of the complexes at room temperature are shown in Figure 4. From the excitation spectrum of **4** (Figure 4a), it can be seen that the ligand-localized ($S_0 \rightarrow S_1$) excitation band is less intense than the $^7F_{0,1}$ and $^5D_0$, $^5G_{0-4}$, $^5L_6$, $^5D_{2,1}$ excitation band,[19] which proves that luminescence sensitization via direct excitation of the europium(III) ion absorption level is much more efficient than the excitation of the ligand. The appearance of the symmetry-forbidden emission $^5D_0 \rightarrow {}^7F_0$ at 579 nm indicates that Eu(III) ions in **4** occupy sites with low

symmetry and have no inversion center,[20] which is further confirmed by the intensity ratio of about 3.1 for $I(^5D_0 \rightarrow {}^7F_2)/I(^5D_0 \rightarrow {}^7F_1)$;[21] this is consistent with the crystallographic analysis. For **6**, the excitation spectrum exhibits a broad excitation band (BEB) between 280 and 400 nm (Figure 4b), indicating that Tb(III) luminescence is efficiently sensitized by the ligand. There are four characteristic peaks, which are assigned to the $^5D_4 \rightarrow {}^7F_J$ (J = 6, 5, 4, 3) transitions. For **7** and **3** (Figure 4c,d), the characteristic emission bands can also be observed in the emission spectra. The overall luminescence quantum yields, $\Phi_{overall}$, of **3**, **4**, **6**, and **7** in the solid state were found to be 1.0, 2.2, 4.5, and 8.6% using an integrating sphere when excited at 325, 325, 324, and 325 nm, respectively. The luminescence lifetime values of **3**, **4**, **6**, and **7** were determined to be 0.066 ± 0.001, 1.013 ± 0.001, 1.427 ± 0.001, and 0.092 ± 0.001 ms from the luminescent decay profiles at room temperature by fitting with a monoexponential curve (Figures S3−S6 in the Supporting Information), indicating the presence of single chemical environment around the emitting Ln(III) ion.

Comparing the emission spectra of these four complexes, we could find that the relative intensity and overall luminescence quantum yield follow the trend **6** > **7** > **4** > **3**, which means that the energy transfer from the ligands to Tb(III) and Dy(III) is more effective than that to Eu(III) and Sm(III) ions. This behavior can be rationalized by the ligand-to-metal energy transfer processes discussed below.

Energy Transfer Processes Studies. To elucidate the energy transfer processes of the lanthanide complexes, the energy levels of the relevant electronic states of the ligand have been investigated. The singlet and triplet energy levels of the ligand were estimated by referring to their wavelengths of UV−vis absorbance edges and the lower wavelength emission edges of the corresponding phosphorescence spectra. The singlet energy level (S_1) of ligand is 32258 cm^{-1} (310 nm) (Figure S7 in the Supporting Information). A triplet excited state T_1 datum of the ligand L is 24213 cm^{-1} ^{2g} (Figure S8 in the Supporting Information), which was calculated by the low-temperature (77 K) phosphorescence spectrum of the Gd(III) complex in a 1:1 methanol−ethanol mixture.[22] According to Reinhoudt's empirical rule,[23] the intersystem crossing process becomes effective when ΔE ($S_1 - T_1$) is at least 5000 cm^{-1}. The energy gap $\Delta E(S_1 - T_1)$ for the ligand is 8045 cm^{-1}. Thus, the intersystem crossing is effective in this ligand. On the other hand, the efficiency of the lowest triplet state (T_1) of the ligand to central ions (antenna effect) is crucial for the sensitization of lanthanide luminescence since the lanthanide ion emissive states must be efficiently populated for emission to occur.

4209

dx.doi.org/10.1021/cg200816f |*Cryst. Growth Des.* 2011, 11, 4205–4212
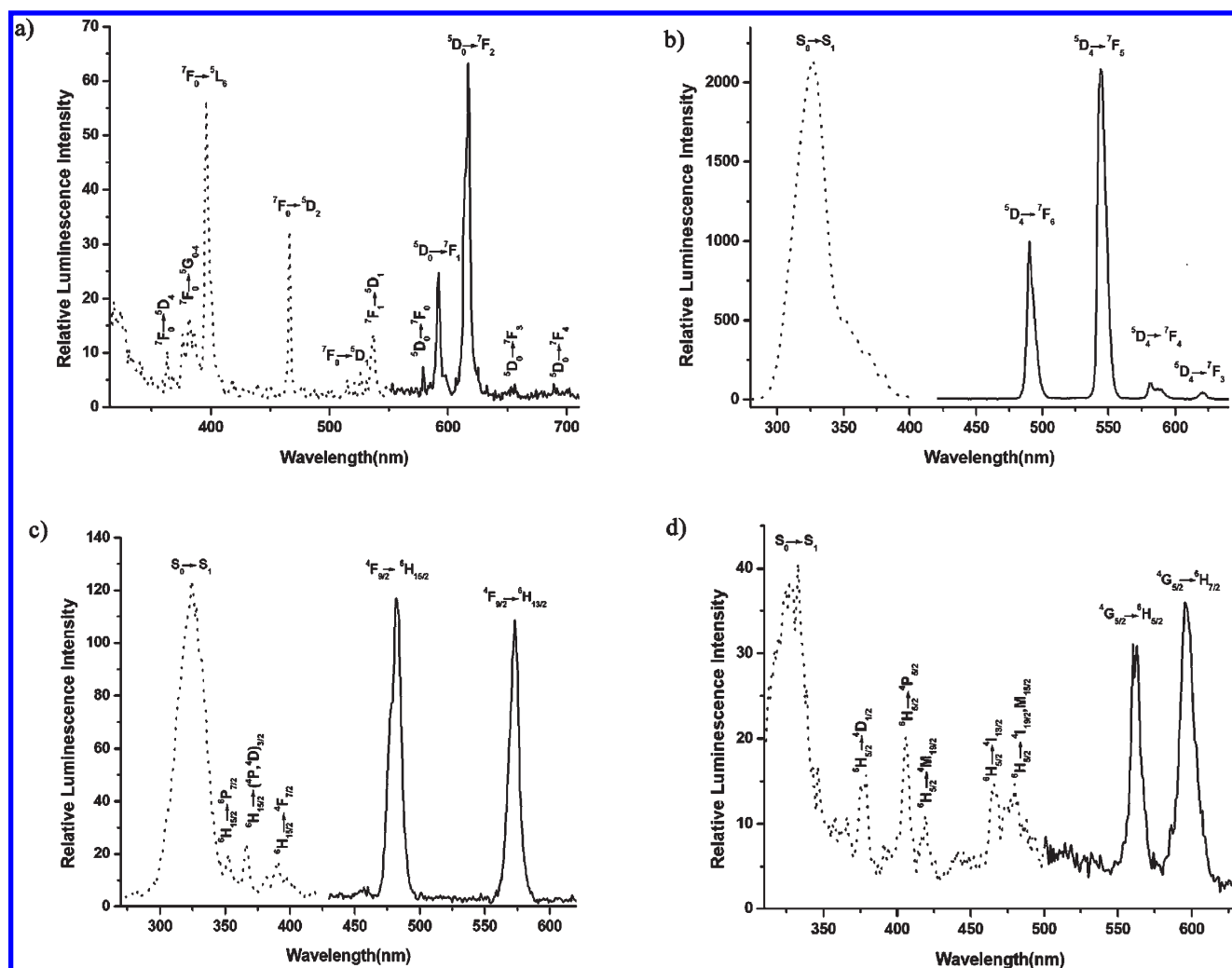
Figure 4. Room temperature excitation and emission spectra of (a) **4** (λ_{ex} = 396 nm), (b) **6** (λ_{ex} = 324 nm), (c) **7** (λ_{ex} = 325 nm), and (d) **3** (λ_{ex} = 325 nm) in the solid state.

It is therefore necessary that there exists a suitable energy gap between the ligand-centered triplet state and the lanthanide ion emissive states. Latva's empirical rule[24] states that an optimal ligand-to-metal energy transfer process for Ln(III) needs $[\Delta E = E(T_1) - E(^5D_J)]$ 2500–4000 cm^{-1} for Eu(III) and 2500–4500 cm^{-1} for Tb(III). The experimentally observed (T_1) energy level of the ligand is 3713 cm^{-1} higher than the $^5D_4$ level of Tb(III) (20500 cm^{-1}) and 3213 cm^{-1} higher than the $^4F_{9/2}$ level of Dy(III) (21000 cm^{-1}), which facilitates efficient energy transfer.[25] By contrast, their energy gaps between ligand and metal-centered levels are 6913 cm^{-1} for Eu(III) $[E(^5D_0) = 17300$ cm$^{-1}]$ and 6313 cm^{-1} for Sm(III) $[E(^4G_{5/2}) = 17900$ cm$^{-1}]$, respectively. Following the method described in literature,[26] it is possible to evaluate the sensitization efficiency of the ligand (η_{sens}) as 7.6% on the basis of the luminescence data (emission spectrum and $^5D_0$ lifetime) (Table S4 in the Supporting Information). The poor sensitization efficiency of the ligand (η_{sens}) indicated that the Eu(III) luminescence is not efficiently sensitized by the ligand. This therefore supports the observation of stronger sensitization of **6** and **7** than **3** and **4**.

■ CONCLUSIONS

In this paper, we report the assembly, crystal structures, and luminescent properties of the lanthanide nitrates coordination polymers with an amide type semirigid bridging ligand 1,3-bis{[(2′-benzylaminoformyl)phenoxyl]methyl}benzene (L). The complexes $\{[Pr_2L_3(NO_3)_6]_n \cdot 4H_2O\}_n$ (**1**) and $\{[Nd_2L_3(NO_3)_6] \cdot 7H_2O\}_n$ (**2**) show unusual porous noninterpenetrated 2D (6,3) nets constructed by Ln(III) ions and the ligand. However, the complexes $[Sm_2L_3(NO_3)_6]_n$ (**3**), $[Eu_2L_3(NO_3)_6]_n$ (**4**), $[Tb_2L_3(NO_3)_6]_n$ (**6**), and $[Er_2L_3(NO_3)_6]_n$ (**8**) demonstrate novel 1D coordination polymeric structures comprised of rings connected by chains. The structure variations from the 2D porous frameworks to the 1D coordination polymeric structures are attributed to the lanthanide contraction effect. On the other hand, the complexes of Sm(III) (**3**), Eu(III) (**4**), Tb(III) (**6**), and Dy(III) (**7**) exhibit characteristic lanthanide-centered luminescence, and the transition intensity changes in the order of **6** > **7** > **4** > **3**, which shows the energy transfer from the ligands to Tb(III) and Dy(III) are more effective than that to Eu(III) and Sm(III). In addition, the ligand-to-metal energy transfer processes studies also make it rational. The successful synthesis of the eight coordination polymers provides a valuable approach for the construction of other lanthanide coordination polymers tuned by lanthanide contraction effect. From a more general perspective, the Tb(III) complex may have the potential application as a light conversion molecular device in many photonic applications.

■ ASSOCIATED CONTENT

ⓢ Supporting Information. Theoretical details of electronic absorption spectra, the intrinsic quantum yield of the Eu(III) complex, tables of selected bond distances and angles, hydrogen bonds in crystal packing of the complexes, the TGA curve and variable-temperature PXRD patterns of the compound **1**, luminescence decay curves of the complexes, absorption spectra of the ligand, phosphorescence spectrum of the compound $[Gd_2L_3(NO_3)_6]\cdot 2H_2O$, and crystallographic data in CIF format. This material is available free of charge via the Internet at http://pubs.acs.org.

■ AUTHOR INFORMATION

Corresponding Author

*Tel: +86-931-8912552. Fax: +86-931-8912582. E-mail: tangyu@lzu.edu.cn.

■ ACKNOWLEDGMENT

■ REFERENCES

(1) (a) Pan, L.; Sander, M. B.; Huang, X.; Li, J.; Smith, M.; Bittner, E.; Bockrath, B.; Johnson, J. K. *J. Am. Chem. Soc.* **2004**, *126*, 1308–1309. (b) Chae, H. K.; Siberio-Perez, D. Y.; Kim, J.; Go, Y.; Eddaoudi, M.; Matzger, A. J.; O'Keeffe, M.; Yaghi, O. M. *Nature* **2004**, *427*, 523–527. (c) Rosi, N. L.; Eckert, J.; Eddaoudi, M.; Vodak, D. T.; Kim, J.; O'Keeffe, M.; Yaghi, O. M. *Science* **2003**, *300*, 1127–1129. (d) Férey, G.; Latroche, M.; Serre, C.; Millange, F.; Loiseau, T.; Percheron-Guégan, A. *Chem. Commun.* **2003**, 2976–2977. (e) Seo, J. S.; Whang, D.; Lee, H.; Jun, S. I.; Oh, J.; Jeon, Y. J.; Kim, K. *Nature* **2000**, *404*, 982–986. (f) Noro, S.-i.; Kitagawa, S.; Kondo, M.; Seki, K. *Angew. Chem., Int. Ed.* **2000**, *39*, 2081–2084. (g) Beauvais, L. G.; Shores, M. P.; Long, J. R. *J. Am. Chem. Soc.* **2000**, *122*, 2763–2772. (h) Hupp, J. T.; Poeppelmeier, K. R. *Science* **2005**, *309*, 2008–2009. (i) Pan, L.; Liu, H.; Lei, X.; Huang, X.; Olson, D. H.; Turro, N. J.; Li, J. *Angew. Chem., Int. Ed.* **2003**, *42*, 542–546. (j) Compton, N. *Chem.—Eur. J.* **2002**, *8*, 3–4. (k) Min, K. S.; Suh, M. P. *Chem.—Eur. J.* **2001**, *7*, 303–313. (l) Min, K. S.; Suh, M. P. *J. Am. Chem. Soc.* **2000**, *122*, 6834–6840. (m) Sawaki, T.; Aoyama, Y. *J. Am. Chem. Soc.* **1999**, *121*, 4793–4798. (n) Fujita, M.; Kwon, Y. J.; Washizu, S.; Ogura, K. *J. Am. Chem. Soc.* **1994**, *116*, 1151–1152. (o) Nijem, N.; Veyan, J.-F.; Kong, L.; Li, K.; Pramanik, S.; Zhao, Y.; Li, J.; Langreth, D.; Chabal, Y. J. *J. Am. Chem. Soc.* **2010**, *132*, 1654–1664. (p) Jiang, H.-L.; Tatsu, Y.; Lu, Z.-H.; Xu, Q. *J. Am. Chem. Soc.* **2010**, *132*, 5586–5587. (q) Zhao, D.; Yuan, D.-Q.; Sun, D.-F.; Zhou, H.-C. *J. Am. Chem. Soc.* **2009**, *131*, 9186–9188. (r) Yazaydin, A. Ö; Snurr, R. Q.; Park, T.-H.; Koh, K.; Liu, J.; LeVan, M. D.; Benin, A. I.; Jakubczak, P.; Lanuza, M.; Galloway, D. B.; Low, J. J.; Willis, R. R. *J. Am. Chem. Soc.* **2009**, *131*, 18198–18199.

(2) (a) Huang, W.; Wu, D.-Y.; Zhou, P.; Yan, W.-B.; Guo, D.; Duan, C.-Y.; Meng, Q.-J. *Cryst. Growth Des.* **2009**, *9*, 1361–1369. (b) Soares-Santos, P. C. R.; Cunha-Silva, L.; Paz, F. A. A.; Ferreira, R. A. S.; Rocha, J.; Trindade, T.; Carlos, L. D.; Nogueira, H. I. S. *Cryst. Growth Des.* **2008**, *8*, 2505–2516. (c) Goff, G. S.; Cisneros, M. R.; Kluk, C.; Williamson, K.; Scott, B.; Reilly, S.; Runde, W. *Inorg. Chem.* **2010**, *49*, 6558–6564. (d) Li, M.-Y.; Lan, Y.; Ako, A. M.; Wernsdorfer, W.; Anson, C. E.; Buth, G.; Powell, A. K.; Wang, Z.; Gao, S. *Inorg. Chem.* **2010**, *49*, 11587–11594.

(e) Ma, S.-Q.; Yuan, D.-Q.; Wang, X.-S.; Zhou, H.-C. *Inorg. Chem.* **2009**, *48*, 2072–2077. (f) Li, X.; Zhang, Y.-B.; Shi, M.; Li, P.-Z. *Inorg. Chem. Commun.* **2008**, *11*, 869–872. (g) Liu, D.-Y.; Kou, Z.-Q.; Li, Y.-F.; Tang, K.-Z.; Tang, Y.; Liu, W.-S.; Tan, M.-Y. *Inorg. Chem. Commun.* **2009**, *12*, 461–464. (h) Ananias, D.; Kostova, M.; Paz, F. A. A.; Neto, A. N. C.; De Moura, R. T.; Malta, O. L.; Carlos, L. D.; Rocha, J. *J. Am. Chem. Soc.* **2009**, *131*, 8620–8626. (i) Abrahams, B. F.; Moylan, M.; Orchard, S. D.; Robson, R. *CrystEngComm* **2003**, *5*, 313–317.

(3) (a) Zhang, Z.-H.; Song, Y.; Okamura, T.-a.; Hasegawa, Y.; Sun, W.-Y.; Ueyama, N. *Inorg. Chem.* **2006**, *45*, 2896–2902. (b) Nag, A.; Schmidt, P. J.; Schnick, W. *Chem. Mater.* **2006**, *18*, 5738–5745. (c) Rudzinski, C. M.; Young, A. M.; Nocera, D. G. *J. Am. Chem. Soc.* **2002**, *124*, 1723–1727. (d) Nozary, H.; Piguet, C.; Rivera, J.-P.; Tissot, P.; Morgantini, P.-Y.; Weber, J.; Bernardinelli, G.; Bünzli, J.-C. G.; Deschenaux R.; Donnio, B.; Guillon, D. *Chem. Mater.* **2002**, *14*, 1075–1090. (e) Binnemans, K.; Görller-Walrand, C. *Chem. Rev.* **2002**, *102*, 2303–2346.

(4) (a) Zucchi, G.; Ferrand, A.-C.; Scopelliti, R.; Bünzli, J.-C. G. *Inorg. Chem.* **2002**, *41*, 2459–2465. (b) Parker, D.; Dickins, R. S.; Puschmann, H.; Crossland, C.; Howard, J. A. K. *Chem. Rev.* **2002**, *102*, 1977–2010. (c) Gawryszewska, P.; Jerzykiewicz, L.; Pietraszkiewicz M.; Legendziewicz, J.; Riehl, J. P. *Inorg. Chem.* **2000**, *39*, 5365–5372.

(5) (a) Marques, N.; Sella, A.; Takats, J. *Chem. Rev.* **2002**, *102*, 2137–2160. (b) Bretonnière, Y.; Wietzke, R.; Lebrun, C.; Mazzanti, M.; Pécaut, J. *Inorg. Chem.* **2000**, *39*, 3499–3505.

(6) Magennis, S. W.; Parsons, S.; Pikramenou, Z. *Chem.—Eur. J.* **2002**, *8*, 5761–5771.

(7) (a) Petoud, S.; Cohen, S. M.; Bünzli, J.-C. G.; Raymond, K. N. *J. Am. Chem. Soc.* **2003**, *125*, 13324–13325. (b) Yan, X.-H.; Cai, Z.-H.; Yi, C.-L.; Liu, W.-S.; Tan, M.-Y.; Tang, Y. *Inorg. Chem.* **2011**, *50*, 2346–2353. (c) Guo, Y.-L.; Dou, W.; Zhou, X.-Y.; Liu, W.-S.; Qin, W.-W.; Zang, Z.-P.; Zhang, H.-R.; Wang, D.-Q. *Inorg. Chem.* **2009**, *48*, 3581–3590. (d) Wang, Q.; Tang, K.-Z.; Liu, W.-S.; Tang, Y.; Tan, M.-Y. *Eur. J. Inorg. Chem.* **2010**, *2010*, 5318–5325. (e) Song, X.-Q.; Zhou, X.-Y.; Liu, W.-S.; Dou, W.; Ma, J.-X.; Tang, X.-L.; Zheng, J.-R. *Inorg. Chem.* **2008**, *47*, 11501–11513.

(8) (a) Wells, A. F. *Three-Dimensional Nets and Polyhedra*; Wiley-Interscience: New York, 1977. (b) Prior, T. J.; Bradshaw, D.; Teatb, S. J.; Rosseinsky, M. J. *Chem. Commun.* **2003**, 500–501.

(9) (a) Wang, Q.; Tang, K.-Z.; Liu, W.-S.; Tang, Y.; Tan, M.-Y. *J. Solid State Chem.* **2009**, *182*, 3118–3124. (b) Guo, S.-P.; Guo, G.-C.; Wang, M.-S.; Zou, J.-P.; Zeng, H.-Y.; Cai, L.-Z.; Huang, J.-S. *Chem. Commun.* **2009**, 4366–4368.

(10) (a) Pan, L.; Huang, X.; Li, J.; Wu, Y.; Zheng, N. *Angew. Chem., Int. Ed.* **2000**, *39*, 527–530. (b) Dimos, A.; Tsaousis, D.; Michaelides, A.; Skoulika, S.; Golhen, S.; Ouahab, L.; Didierjean, C.; Aubry, A. *Chem. Mater.* **2002**, *14*, 2616–2622. (c) Zhuang, G.-L.; Kong, X.-J.; Long, L.-S.; Huang, R.-B.; Zheng, L.-S. *CrystEngComm* **2010**, *12*, 2691–2694. (d) Wang, Y.-W.; Zhang, Y.-L.; Dou, W.; Zhang, A.-J.; Qin, W.-W.; Liu, W.-S. *Dalton Trans.* **2010**, *39*, 9013–9021. (e) Lu, W.-G.; Jiang, L.; Lu, T.-B. *Cryst. Growth Des.* **2010**, *10*, 4310–4318. (f) Deng, Z.-P.; Kang, W.; Huo, L.-H.; Zhao, H.; Gao, S. *Dalton Trans.* **2010**, *39*, 6276–6284. (g) Wang, Z.-H.; Fan, J.; Zhang, W.-G. *Z. Anorg. Allg. Chem.* **2009**, *635*, 2333–2339. (h) Wan, Y.-H.; Zheng, X.-J.; Wang, F.-Q.; Zhou, X.-Y.; Wang, K.-Z.; Jin, L.-P. *CrystEngComm* **2009**, *11*, 278–283. (i) Ma, S.; Yuan, D.; Wang, X.-S.; Zhou, H.-C. *Inorg. Chem.* **2009**, *48*, 2072–2077. (j) Liu, M.-S.; Yu, Q.-Y.; Cai, Y.-P.; Su, C.-Y.; Lin X.-M.; Zhou, X.-X.; Cai, J.-W. *Cryst. Growth Des.* **2008**, *8*, 4083–4091. (k) Kong, X.-J.; Ren, Y.-P.; Long, L.-S.; Huang, R.-B.; Zheng, L.-S.; Kurmoo, M. *CrystEngComm* **2008**, *10*, 1309–1314. (l) Xia, J.; Zhao, B.; Wang, H.-S.; Shi, W.; Ma, Y.; Song, H.-B.; Cheng, P.; Liao, D.-Z.; Yan, S.-P. *Inorg. Chem.* **2007**, *46*, 3450–3458. (m) Wang, S.-N.; Sun, R.; Wang, X.-S.; Li, Y.-Z.; Pan, Y.; Bai, J.; Scheer, M.; You, X.-Z. *CrystEngComm* **2007**, *9*, 1051–1061. (n) Seitz, M.; Oliver, A. G.; Raymond, K. N. *J. Am. Chem. Soc.* **2007**, *129*, 11153–11160. (o) Cheng, J.-W.; Zheng, S.-T.; Yang, G.-Y. *Dalton Trans.* **2007**, 4059–4066. (p) Li, X.-F.; Han, Z.-B.; Cheng, X.-N.; Chen, X.-M. *Inorg. Chem. Commun.* **2006**, *9*, 1091–1095. (q) He, Z.; Gao, E.-Q.; Wang, Z.-M.; Yan, C.-H.;

Kurmoo, M. *Inorg. Chem.* **2005**, *44*, 862–874. (r) Sun, H.-L.; Ye, C.-H.; Wang, X.-Y.; Li, J.-R.; Gao, S.; Yu, K.-B. *J. Mol. Struct.* **2004**, *702*, 77–83. (s) Mizukami, S.; Houjou, H.; Kanesato, M.; Hiratani, K. *Chem.—Eur. J.* **2003**, *9*, 1521–1528. (t) Liu, Q.-D.; Gao, S.; Li, J.-R.; Ma, B.-Q.; Zhou, Q.-Z.; Yu, K.-B. *Polyhedron* **2002**, *21*, 1097–1103.

(11) Kondo, M. *Bull. Chem. Soc. Jpn.* **1976**, *49*, 2679–2682.

(12) (a) Sheldrick, G. M. *Acta Crystallogr. A* **1990**, *46*, 467–473. (b) Sheldrick, G. M. *SHELXS-97, A Program for X-ray Crystal Structure Solution, and SHELXL-97, A Program for X-ray Structure Refinement*; Göttingen University: Germany, 1997.

(13) (a) Wang, Y.-L.; Yuan, D.-Q.; Bi, W.-H.; Li, X.; Li, X.-J.; Li, F.; Cao, R. *Cryst. Growth Des.* **2005**, *5*, 1849–1855. (b) Prior, T. J.; Rosseinsky, M. J. *Chem. Commun.* **2001**, 495–496.

(14) Spek, A. L. *PLATON*; Utrecht University: Utrecht, The Netherlands, 2003.

(15) Sabbatini, N.; Guardigli, M.; Lehn, J.-M. *Coord. Chem. Rev.* **1993**, *123*, 201–228.

(16) Jørgenson, C. K. *Prog. Inorg. Chem.* **1962**, *4*, 73–124.

(17) (a) Aiga, F.; Iwanaga, H.; Amano, A. *J. Phys. Chem. A* **2005**, *109*, 11312–11316. (b) He, P.; Wang, H.-H.; Liu, S.-G.; Shi, J.-X.; Wang, G.; Gong, M.-L. *Inorg. Chem.* **2009**, *48*, 11382–11387. (c) Regulacio, M. D.; Pablico, M. H.; Vasquez, J. A.; Myers, P. N.; Gentry, S.; Prushan, M.; Tam-Chang, S.-W.; Stoll, S. L. *Inorg. Chem.* **2008**, *47*, 1512–1523.

(18) (a) de Sá, G. F.; Malta, O. L.; de Mello Donegá, C.; Simas, A. M.; Longo, R. L.; Santa-Cruz, P. A.; da Silva, E. F. *Coord. Chem. Rev.* **2000**, *196*, 165–195. (b) Bazzicalupi, C.; Bencini, A.; Bianchi, A.; Giorgi, C.; Fusi, V.; Masotti, A.; Valtancoli, B.; Roque, A.; Pina, F. *Chem. Commun.* **2000**, 561–562.

(19) (a) Shyni, R.; Biju, S.; Reddy, M. L. P.; Cowley, A. H.; Findlater, M. *Inorg. Chem.* **2007**, *46*, 11025–11030. (b) Biju, S.; Raj, D. B. A.; Reddy, M. L. P.; Kariuki, B. M. *Inorg. Chem.* **2006**, *45*, 10651–10660.

(20) (a) Sun, Y.-Q.; Zhang, J.; Yang, G.-Y. *Chem. Commun.* **2006**, 4700–4702. (b) Bünzli, J.-C. G.; Piguet, C. *Chem. Soc. Rev.* **2005**, *34*, 1048–1077.

(21) Kirby, A. F.; Foster, D.; Richardson, F. S. *Chem. Phys. Lett.* **1983**, *95*, 507–512.

(22) Dawson, W. R.; Kropp, J. L.; Windsor, M. W. *J. Chem. Phys.* **1966**, *45*, 2410–2418.

(23) Steemers, F. J.; Verboom, W.; Reinhoudt, D. N.; van der Tol, E. B.; Verhoeven, J. W. *J. Am. Chem. Soc.* **1995**, *117*, 9408–9414.

(24) (a) Latva, M.; Takalo, H.; Mukkala, V.-M.; Matachescu, C.; Rodríuez-Ubis, J. C.; Kankare, J. *J. Lumin.* **1997**, *75*, 149–169. (b) Arnaud, N.; Georges, J. *Spectrochim. Acta* **2003**, *59*, 1829–1840.

(25) Gutierrez, F.; Tedeschi, C.; Maron, L.; Daudey, J.-P.; Poteau, R.; Azema, J.; Tisnès, P.; Picard, C. *Dalton Trans.* **2004**, 1334–1347.

(26) (a) Eliseeva, S. V.; Bünzli, J.-C. G. *Chem. Soc. Rev.* **2010**, *39*, 189–227. (b) Werts, M. H. V.; Jukes, R. T. F.; Verhoeven, J. W. *Phys. Chem. Chem. Phys.* **2002**, *4*, 1542–1548. (c) Fernandes, M.; de Zea Bermudez, V.; Sá Ferreira, R. A.; Carlos, L. D.; Charas, A.; Morgado, J.; Silva, M. M.; Smith, M. J. *Chem. Mater.* **2007**, *19*, 3892–3901.